6-30-2016

PVDF Membranes with Stable, Ultrathin Graphene Oxide (GO) Functional Coatings for Antifouling Oil/Water Separation under Cross-Flow Condition

Lei Wang
University of South Carolina

PVDF Membranes with Stable, Ultrathin Graphene Oxide (GO) Functional Coatings for Antifouling Oil/Water Separation under Cross-Flow Condition

by

Lei Wang

Bachelor of Engineering
Dalian University of Technology, 2011

Submitted in Partial Fulfillment of the Requirements

For the Degree of Master of Science in

Chemical Engineering

College of Engineering and Computing

University of South Carolina

2016

Accepted by:

Miao Yu, Director of Thesis

John R. Regalbuto, Reader

Christopher Williams, Reader

John W. Weidner, Reader

Lacy Ford, Senior Vice Provost and Dean of Graduate Studies

DEDICATION

This dissertation work is dedicated to my parents.

ACKNOWLEDGEMENTS

I would like to give my greatest acknowledgement to my advisor, Dr. Miao Yu, for his novel ideas and kind guidance throughout my research projects. Both my experimental skills and theoretical knowledge have been significantly enriched during our daily discussion and interaction. Sincere thanks also go to my MS committee members, Dr. John R. Regalbuto and Christopher Williams, for their precious advices.

I also want to thank all of my friends in USC, who not only offered me academic assistance during my research and study, but also helped me in my personal life. We had a lot of fun together in the past years, and it will become the one of the most valuable memories in my overseas experience.

Last but not least, I am truthfully grateful to my parents, for their love, caring, support and understanding. You always stood by me and encouraged me during these years. I feel really happy to have you as a family.

ABSTRACT

Oil/water separation plays an important role in industrial wastewater treatment and environment protection. For the treatment of oily wastewater, especially for removing oil droplets with sizes in the micrometer range, ultrafiltration (UF) membrane technology is considered the most efficient method due to its high separation efficiency and relatively simple operational process. However, caused by the deposition of the oil droplets onto the membrane surface and into the membrane pores, the fouling of UF membranes shortens their service time and degrades their separation performance in practical applications.

In this work, graphene oxide (GO) was utilized as a novel coating material to modify PVDF membranes, by a similar vacuum filtration method for antifouling oil/water separation. PVDF membranes with ultrathin GO coatings showed improved hydrophilicity and under water oleophobicity and thus minimized underwater oil adhesion on the membrane surface. And the oil/water separation results showed that by optimization of the GO coating thickness, greatly improved antifouling performance could be achieved. As a result, the separation flux with GO coatings was at least doubled, compared with PVDF membrane itself. The novel GO functional coatings with optimized thickness may have great potential for antifouling oil/water separation.

TABLE OF CONTENTS

LIST OF FIGURES

LIST OF ABBREVIATIONS

AFM ..... Atomic Force Microscopy

CA ..... Contact Angle

FESEM ..... Field Emission Scanning Electron Microscopy

GO ..... Graphene Oxide

HD ..... Hexadecane

MF ..... Microfiltration

NF ..... Nanofiltration

PHC ..... Petroleum Hydrocarbons

PVDF ..... Polyvinylidene Fluoride

PA ..... Polyamide

Rq ..... Root-mean-squared Roughness

SDS ..... Sodium Dodecyl Sulfate

TCD ..... Thermal Conductivity Detector

TOC ..... Total Organic Carbon

UF ..... Ultrafiltration

UV ..... Ultraviolet

UV-vis ..... Ultraviolet-Visible Spectroscopy

XPS ..... X-ray Photoelectron Spectroscopy

XRD ..... X-ray Diffraction

CHAPTER 1

INTRODUCTION

Oil/water separation via highly energy efficient ways has become an urgent need because of the large amount of oily wastewater produced in many industrial processes and daily life. On one hand, oily wastewater, produced by textile, food, steel, leather, petrochemical and metal industries, has caused severe pollution problem all over the world[1,2,3,4]. For example, in agriculture, soil will change its physical and chemical properties when the oily sludge water enters soil; the sludge covers the soil particles permanently and leads to a morphology change of the soil. As a result, the plants that grow on contaminated soil may have low productivity and severely restricted growth. On the other hand, oil spill accidents may happen during the petroleum exploration, refinement and transports, which causes serious environmental pollution and the loss of energy and economy[5,6]. Furthermore, with rapid population growth and steadily worsening of the climate, how to solve the problem of freshwater scarcity has become a serious global issue, especially in certain underdeveloped countries. Therefore, in order to solve these problems, it is important and necessary to develop effective technologies and materials for oil/water separation.

Various methods have been widely used for oil/water separation in industry, and these methods can be classified as physical and chemical methods. Typical physical methods include gravity separation, centrifugation, ultrasonic irradiation separation, adsorption (activated carbon, copolymers and zeolites), and evaporation. Oxidation,

pyrolysis, photocatalytic treatment and ionic liquids at room temperature are chemical treatment methods. These conventional methods have advantages as well as obvious disadvantages.

For example, the centrifugation method is very easy to process; during the whole separation process, there is no need of any solvent and no damage to the environment. However, this method needs a large amount of energy, and it is difficult to settle down the small oil droplets [7]. Ultrasonic irradiation is a fast method, but the cost of the heavy equipment is very high and it is not effective to treat oil/water mixtures with heavy metals. Oxidation and pyrolysis are both rapid and effective chemical methods for oil/water separation, and can treat large capacity of oily sludge and completely remove the petroleum hydrocarbons (PHC). Nonetheless, the treatment cost is high, and they need large space for the designed equipment installation and may generate some secondary pollutants into the environment during separation. In contrast, membrane separation has the great potential as a simple and highly energy efficient oil/water separation technology in 21st century and has been extensively studied and developed in recent years. The main issue in membrane separation is the membrane fouling, which is caused by surfactant adsorption or pore plugging by oil droplets. Fouling could lead to a drastic decline of the water flux and rejection[8,9]. Currently, solving the fouling problem is the main research focus in oil/water separation by membrane separation processes.

1.1 Membrane Separation Technology

Membrane technology has gradually become an important separation technology during the recent few decades. It has been widely applied in various fields, such as gas separation, environmental protection, food industry, and polluted water treatment.

Compared with other separation methods, such as distillation, extraction, and centrifugation, membrane separation process is relative new. Depending on the development stage and application fields , membrane separation can be classified as first generation membrane processes, such as microfiltration (MF), ultrafiltration (UF), nanofiltration (NF), reverse osmosis (RO), membrane electrodialysis (ED), and membrane electrolysis (ME), and second generation membrane processes, such as gas separation (GS), pervaporation (PV), membrane distillation (MD), and carrier mediated processes[10].

Membrane is the core of every membrane separation processes. It can be defined as a selective barrier or semi-permeable interface which can separate two different phases, block the permeation of various materials based on specific properties, and control the permeation rate of the species passing through the membrane. Thickness of a membrane is over a wide range from less than 10 nm to as thick as several hundred micrometers. Transport through a membrane is usually driven by chemical potential differences between feed and permeate resulting from the concentration, pressure and temperature gradients. Moreover, a membrane can be natural or synthetic, neutral or charged[10]. Compared with traditional separation methods, membrane separation process is much simpler and needs low energy input without addition of chemicals. Therefore, membranes are becoming more popular in oil/water separation.

Figure 1 is a schematic of membrane separation process. The influent of a defined as the volume permeating through the membrane per unit area and time. Flux through a membrane can be calculated by the following equation[10]:

$$J_I = -A_i \frac{dX_i}{dx}$$

Where Ji is the flux of the component i, Ai is the proportionality coefficient of component

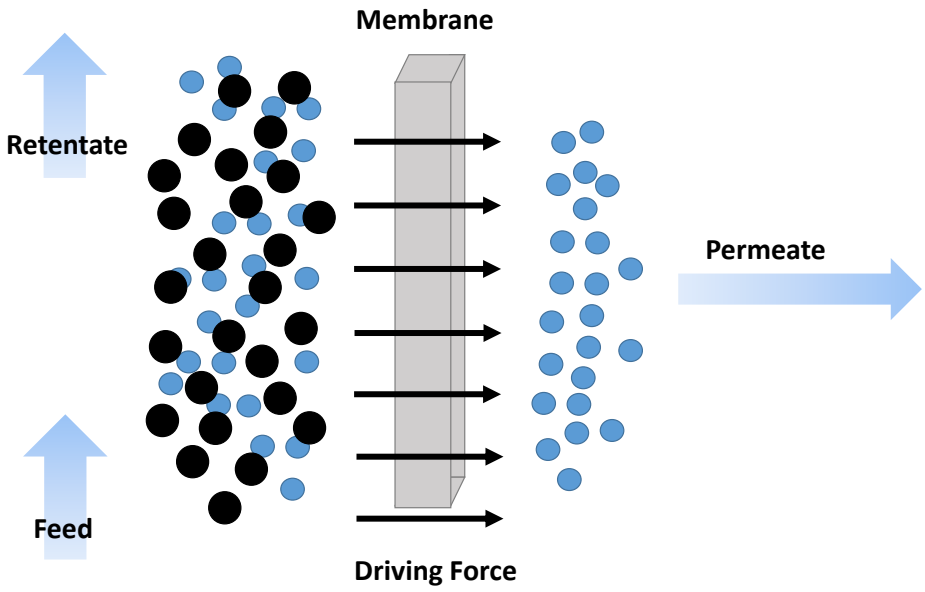

Figure 1.1 Membrane based separation process.

i, and dXi/dx is the driving force which presents the chemical potential gradient of component i along a coordinate x perpendicular to the membrane surface. High flux can significantly reduce total membrane area and capital cost, and thus is desirable for membrane separation processes. Selectivity indicates the capability of a membrane to separate a component from a mixture, and appropriate pore size is needed to provide high enough selectivity and thus realize effective separation. An ideal membrane, therefore, needs to optimize these two important properties so that maximum flux can be obtained while maintaining decent separation selectivity. For dilute aqueous mixtures, consisting of two different liquids which normally are defined as solvent (mostly water) and solute, the selectivity is typically referred to as the retention (R) towards the solute. For oil/water separation, both flux and selectivity of a membrane need to be considered simultaneously. The retention is given by the following equation[10]:

$$R = \frac{c_f - c_p}{c_f} = 1 - \frac{c_p}{c_f}$$

Where c_f is the solute concentration in the feed, and c_p is the solute concentration in the permeate. The value of R varies between 100% (complete retention of the solute: this situation is defined as an "ideal" semipermeable membrane) and 0% (solute and solvent pass through the membrane freely).

Based on the different physical and chemical properties, membrane can generally be classified as isotropic and anisotropic, microporous and nonporous (dense) membranes, electrically charged membranes, or inorganic and organic membranes[11], as shown schematically in Fig. 2. Microporous membranes have a highly uniform structure with randomly interconnected pores, and the range of these pores are from 0.01 to 10 μm in diameter. The separation process of microporous membrane is dependent on the distribution of molecular size and pore size, and molecules or particles with a size difference can be separated effectively. Nonporous, dense membranes are usually composed of a thin layer of dense material. The separation of a mixture is affected by the diffusivity and solubility of the components in the membrane material, which makes it possible for dense membranes to separate the mixture with similar size if their concentration in the membrane is enormously different from others. Dense membranes are now widely used in industry for gas separation, pervaporation and reverse osmosis, and usually these membranes improve their flux by forming an anisotropic structure with another membrane. Electrically charged membranes are also referred to as ion-exchange membranes, the separation of these membranes is achieved mainly by moving ion from one solution to another, and the excluded ions is depended on the charge of the fixed ions of the membrane structure. These membranes are used for processing electrolyte solution in ED. Inorganic membranes are the membranes made of materials, such as carbon[13],

silica[14], zeolites[15] and metals[16], while organic membranes are polymeric[17] membranes, such as polyvinylidene fluoride (PVDF)[18] and polyamide (PA)[19]. However, these classifications are not very independent, because some membranes might not belong to only one category. For example, inorganic and polymeric membranes can be either microporous or dense. Carbon, silica, zeolites and some polymeric membranes are porous, while metal membranes are dense. Electrical charged membranes can be porous or dense, but are most commonly microporous. Most microporous membranes and nonporous membranes are isotropic membranes. An anisotropic membrane is made of an extremely thin film coating on a much thicker, porous substructure. It's a composite membrane and is physically or chemically heterogeneous.

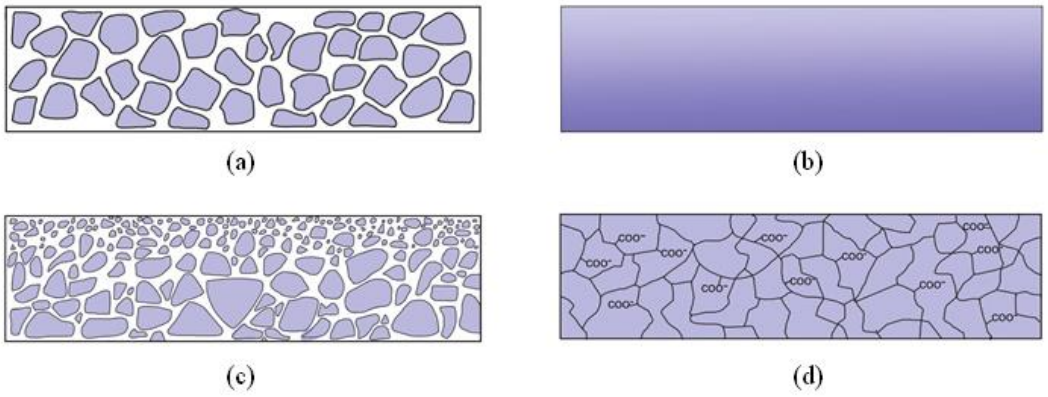

Figure 1.2 The schematic diagrams of the principal types of membranes (a) Isotropic micro-porous membrane; (b) Nonporous (dense) membrane; (c) nanopores membrane (Loeb-Sourirajan anisotropic structure); (d) Electrically charged membrane.

Development of anisotropic membrane manufacture techniques represents a big breakthrough of membrane separation process. In the manufacture, the membranes can be fabricated in large scale with a very low cost[20,21], and the layers are made from different materials. Normally, a much thicker, highly permeable microporous substrate functions as a mechanical support to handle the selective membrane, and the selective membrane

usually is a very thin film with a special physical or chemical property. Theoretically, the thinner the selective membrane is, the higher the flux will be. Because of the significant merits of higher fluxes, the anisotropic membranes are used in almost all commercial and industrial processes, especially for oil/water separation process.

1.2 Anisotropic membrane for oil/water separation

During the last few decades, membrane separation process has been further developed to purify the water/oil emulsion. Membrane filtration has been successfully applied for the separation of stable emulsions, dissolved oil and even organic molecules. However, membrane fouling is the most significant problem needed to solve. It not only reduces selectivity and flux but also greatly increases operation cost[22,23,24]. In recent years, studies on wettability of anisotropic membranes for oil/water separation have attracted great attention and led to remarkable achievements. Wettability is an intrinsic property of a solid surface and represents the interaction between the surface and a liquid. Wettability can be defined by the contact angle of the fluid with the solid surface. Because of the different wetting properties for oil and water, the wettability can be classified as hydrophobic (water-hating) and hydrophilic (water-loving), or oleophobic (oil-hating) and oleophilic (oil-loving). So, by combing any two of the above properties, anisotropic membranes with special wetting surface have been successfully obtained, and a large amount of specially designed materials have been widely applied in the field of oil/water separation.

1.2.1 Ceramic filtration membranes

Ceramic filtration membranes act as an important role in the family of filtration membranes. They have been widely used in industrial processes, especially in some harsh

conditions, such as corrosive and high temperature, pressure environments, because of their high chemical, thermal and mechanical stabilities. What's more, as ceramic membranes have a rigid porous structure, the cleaning can be done with high temperature calcination or harsh chemical (if necessary) without any effect on the membrane performance. Recently, ceramic membranes are employed for oil/water separation by some researchers[25,26,27,28,29,30,31,32,33]. As the pore size of ceramic membranes ranges from macropores (>50 nm) to micropores (< 2 nm), if using ceramic membranes for oil/water separation directly, the oil droplets will block the pores and cause severe fouling problem[27,30].

Up to now, various ceramic filtration membranes, such as zirconia, titania and silica, have been fabricated and applied for oil/water separation. Cui and coworkers prepared a NaA zeolite microfiltration (MF) membrane by using in-situ hydrothermal synthesis method on α-Al_2O_3 tube and investigated the separation performance and recovery for oil/water mixture[29]. It was reported that the NaA/α-Al_2O_3 MF membranes could obtain a high oil rejection of more than 99% with less than 1mg oil /L. Compared with other ceramic membranes, these NaA zeolite membranes exhibited a good antifouling ability, and the separation performance could be maintained for a long period of time because of the strong hydrophilicity of NaA zeolite. Zhou and co-workers modified commercial Al_2O_3 microfiltration membranes to reduce the membrane fouling performance by coating a layer of nano-sized ZrO_2 particles[32]. Because of the high hydrophilicity of ZrO_2, the modified ceramic membranes became more hydrophilic and exhibited an improved flux and a high rejection for oil/water separation; the steady flux kept 88% of the initial flux, and the oil rejection was above 97.8%. In addition to the alumina-based ceramic membranes, other

ceramic membranes, such as zirconia-, zeolite- and polymer-based, were modified to investigate the antifouling performance for oil/water separation[25,30].

1.2.2 Polymer-dominated filtration membranes

Polymers, such as polyvinylidene fluoride (PVDF), polysulfone (PSF) and polyacrylonitrile (PAN), have been widely used in the preparation of microfiltration and ultrafiltration membranes for oil/water separation[34,35,36,37,38]. Due to their high efficiency to remove oil, low energy requirements, superior chemical and mechanical stability, and inexpensive cost, polymer filtration membranes are leading the membrane separation industry market. However, because of the intrinsic property of polymers, most polymer membranes are oleophilic, which easily leads to membrane fouling and causes the flux decline and rejection deterioration for oil/water separation. In order to improve the antifouling performance of polymer filtration membranes, many methods have been employed to synthesize anisotropic structure with hydrophilicity property.

Applying phase inversion process to blend a polymer with hydrophilic materials is a common and effective method to improve the hydrophilicity of polymers. For oil/water separation, improvement of the membrane permeability and antifouling performance is the main purpose for membrane blending. After blending, the isotropic membranes are expected to be more hydrophilic so that the oil droplets are hard to absorb on the membrane surface. Nunes and Peinemann reported that they successfully blended poly (methyl methacrylate) (PMMA) with PVDF together to form the asymmetric membrane for filtration, and the water permeability increased 14-fold without loss of retention by add 1% PMMA to the casting solution[38]. Later, Marchese and co-authors investigated the effect of the PMMA content on the degree of hydrophilicity of PVDF/PMMA blended membranes[34].

It was reported that with the increase of PMMA loading in the blends, both the hydrophilicity and surface porosity increased, and the higher content of PMMA led to a higher water permeability, which could also reduce the fouling performance on the membrane surface.

Surface modification is another method to improve the antifouling performance of membranes. Modification can be made by either chemical (such as grafting, coating and acid base treatment) or physical (plasma irradiation and vaper phase deposition) techniques. Among these techniques, surface coating is a kind of simple process to introduce various hydrophilic layers by dipping or directly adsorbing water-soluble solution onto the membrane surface. However, instability of the coated layers is the main problem needed to solve, and they may be peeled off from the membrane surface during oil/water separation[39]. Freeman and co-workers successfully synthesized potential fouling reducing coating materials by free-radical photopolymerization of aqueous solutions of poly (ethylene glycol) diacrylate (PEGDA), and then used this crosslinked PEGDA to coat on the surface of PSF membranes to form the composite membranes[40]. For crossflow oil/water filtration, the coated PSF membranes had 400% higher water flux than that of an uncoated PSF membrane after 24 h of permeation; the coated membranes also had higher organic rejection than the uncoated membranes. In this work, the water contact angle decreased from 131^0 to 52^0, which means the hydrophilicity of the coated PSF membranes increased drastically, compard with the uncoated PSF membranes. Enhancement of the hydrophilicity of the coated membranes resulted in the reduced fouling by oil/water emulsion. Feng and co-workers used solid-vapor interfacial crosslinking to modify PVDF membranes by coating with a dilute poly (vinyl alcohol) (PVA) aqueous solution[41]. The

fouling tests showed that a short period of coating and crosslinking improved the antifouling performance, and the flux of the modified membrane was twice as high as that of the unmodified membrane after 18h natural water ultrafiltration. They attributed this to the increased the smoothness and hydrophilicity of PVDF membrane.

1.3 Graphene-Based Membranes for Oil/water Separations

Graphite oxide (GO) is typically prepared by treating graphite with strong oxidizing agents, and is a compound of carbon, oxygen and hydrogen[42]. Ratio of carbon to oxygen is variable, which depends on the preparation methods[43,44,45,46], the reaction conditions, and the precursors of graphite[47]. Graphene oxide can be viewed as a one atom thick sheet of graphite oxide, and it is a good candidate for water purification because of its unique permeability of water. The dried GO is amphiphilic[48] and the distance between two individual GO layers is around 0.6nm[49]. However, only water molecules can permeate through the GO layers while other molecules cannot, and the distance between GO flakes increases to 1.2 nm with the increasing humidity [49], which shows that GO is hydrophilic and easily hydrated when exposed to water.

In the past few years, based on the hydrophilicity, GO has been studied and reported for oil/water separation by a lot of researchers. Hu and Mi reported a novel procedure to synthesize GO membrane for water separation[50,51,33,52,53]. Dong and co-workers reported that they easily synthesized a GO composite membrane by immersing stainless steel meshes into GO aqueous solution[51]. Compared to neat meshes, GO coated meshes become more hydrophilic in air and superoleophobic under water. Due to this completely opposite wettability, various oils can be simply and efficiently separated from water by using coated meshes under only a gravity-driven force, and the separation efficiency of GO coated

meshes for water or light oils is above 98%, and above 90% for heavy oils. Li and co-workers prepared superhydrophobic and superoleophilic graphene/polyvinylidene fluoride (GO/PVDF) aerogels by solvothermal reduction of GO and PVDF mixed dispersions[54]. The modified aerogels showed a high absorption capacity for oils and organic solvents, and an excellent absorption recyclability. What is more, their preparation procedure is simple and the cost is very low. Thus, their work not only successfully prepared a promising material for oil/water separation, but also paved a facile way to fabricate superhydrophobic and superoleophilic graphene-based membranes by compositing GO with a hydrophobic polymer. Recently, Hu and co-workers prepared a both high permeate flux and high oil rejection composite ceramic membrane on commercial 19 channels Al_2O_3 ceramic filtration membrane with GO coating[33]. Similarly, due to the high hydrophilic of GO, the GO/Al_2O_3 membrane exhibited a 27.8% higher improvement of flux for oil/water emulsion compared with the Al_2O_3 microfiltration membrane without any GO coating.

1.4 PVDF with GO coating for Oil/water Separations

Recently, our group designed and fabricated a GO ultrafiltration (UF) membrane structure with an optimized hierarchical surface roughness for antifouling oil/water separation[55]. The novel structure was inspired by fish scales which are covered by a thin layer of hydrophilic mucus. The hierarchical surface roughness of fish scales can trap the absorbed water molecules and then form a thin layer of water to function as a composite water-solid interface, which can effectively prevent the adhesion of oil. Moreover, the hierarchical structure can significantly decrease the adhesive force in oil/water/solid systems[56]. So this structured surface will release the oil to the top of the water when contacting with oil/water emulsion, and show excellent antifouling performance. Graphene

oxide is a rising 2D membrane and coating material with high hydrophilicity. We coated the GO on polyamide (PA) by using a facile vacuum filtration method. The GO/PA composite membranes exhibited an excellent antifouling performance and almost 100% pure water flux recovery capability in cyclic oil-in-water emulsion separation tests. Thus, we anticipate the GO coating concept is generic, and can be applied to plenty of other commercially available porous supports with rough surfaces such as PVDF, and may generate a group of underwater superoleophobic membranes with low-oil-adhesion for oil/water separation process. However, in this work, as we used a self-designed stainless-steel dead-end module, the flux of oil/water emulsion decreased during the oil-in-water separation. This is because the oil concentration in the module increased while pure water passed through the membrane. So, in my work here we focused on oil/water separation by GO membranes using a cross-flow filtration apparatus.

The main objective of the thesis is to study the antifouling performance of GO coating materials in oil/water separation by using cross-flow filtration apparatus. In the current work, I firstly finished building the cross-flow system and investigated the effect of feed's flow rate on the antifouling performance of the composite membrane. Then, I tried to coat the GO on a ceramic Al_2O_3 membrane and tested its antifouling performance. At last, I decided to use polyvinylidene fluoride (PVDF) as the support to investigate the antifouling performance of GO coating for oil/water separation in detail.

References

(1) Shi, Z.; Zhang, W.; Zhang, F.; Liu, X.; Wang, D.; Jin, J.; Jiang, L. *Adv. Mater.* **2013**, *25* (17), 2422–2427.

(2) Chan, Y. J.; Chong, M. F.; Law, C. L.; Hassell, D. G. *Chem. Eng. J.* **2009**, *155* (1-2), 1–18.

(3) Ju, H.; McCloskey, B. D.; Sagle, A. C.; Wu, Y.-H.; Kusuma, V. A.; Freeman, B. D. *J. Membr. Sci.* **2008**, *307* (2), 260–267.

(4) Zhang, W.; Shi, Z.; Zhang, F.; Liu, X.; Jin, J.; Jiang, L. *Adv. Mater.* **2013**, *25* (14), 2071–2076.

(5) Kammerer, M.; Mastain, O.; Le Dréan-Quenech'du, S.; Pouliquen, H.; Larhantec, M. *Sci. Total Environ.* **2004**, *333* (1-3), 295–301.

(6) Nordvik, A. B.; Simmons, J. L.; Bitting, K. R.; Lewis, A.; Strøm-Kristiansen, T. *Spill Sci. Technol. Bull.* **1996**, *3* (3), 107–122.

(7) Comba, M.; Kaiser, K. *Sci. Total Environ.* **1990**, *97-98*, 191–206.

(8) Song, L. *J. Membr. Sci.* **1998**, *139* (2), 183–200.

(9) Kong, J.; Li, K. *Sep. Purif. Technol.* **1999**, *16* (1), 83–93.

(10) Mulder, M. *Basic principles of membrane technology*, 2nd ed.; Kluwer Academic: Dordrecht ; Boston, 1996.

(11) Baker, R. W. *Membrane technology and applications*; J. Wiley: Chichester; New York, 2004.

(12) Peng, X.; Jin, J.; Nakamura, Y.; Ohno, T.; Ichinose, I. *Nat. Nanotechnol.* **2009**, *4* (6), 353–357.

(13) Shiflett, M. B. *Science* **1999**, *285* (5435), 1902–1905.

(14) de Vos, R. M. *Science* **1998**, *279* (5357), 1710–1711.

(15) Caro, J.; Noack, M.; Kölsch, P.; Schäfer, R. *Microporous Mesoporous Mater.* **2000**, *38* (1), 3–24.

(16) Athayde, A. L.; Baker, R. W.; Nguyen, P. *J. Membr. Sci.* **1994**, *94* (1), 299–311.

(17) Park, H. B.; Jung, C. H.; Lee, Y. M.; Hill, A. J.; Pas, S. J.; Mudie, S. T.; Van Wagner, E.; Freeman, B. D.; Cookson, D. J. *Science* **2007**, *318* (5848), 254–258.

(18) Wang, D.; Li, K.; Teo, W. . *J. Membr. Sci.* **1999**, *163* (2), 211–220.

(19) Elimelech, M.; Xiaohua Zhu; Childress, A. E.; Seungkwan Hong. *J. Membr. Sci.* **1997**, *127* (1), 101–109.

(20) Ho, W. S. W.; Sirkar, K. K. *Membrane Handbook*; Springer US: Boston, MA, 1992.

(21) Freemantle, M. *Chem. Eng. News* **2005**, *83* (40), 49–57.

(22) Toyoda, M.; Inagaki, M. *Carbon* **2000**, *38* (2), 199–210.

(23) Gupta, V. K.; Carrott, P. J. M.; Ribeiro Carrott, M. M. L.; Suhas. *Crit. Rev. Environ. Sci. Technol.* **2009**, *39* (10), 783–842.

(24) Cheryan, M.; Rajagopalan, N. *J. Membr. Sci.* **1998**, *151* (1), 13–28.

(25) Faibish, R. S.; Cohen, Y. *Colloids Surf. Physicochem. Eng. Asp.* **2001**, *191* (1-2), 27–40.

(26) Faibish, R. *J. Membr. Sci.* **2001**, *185* (2), 129–143.

(27) Hua, F. L.; Tsang, Y. F.; Wang, Y. J.; Chan, S. Y.; Chua, H.; Sin, S. N. *Chem. Eng. J.* **2007**, *128* (2-3), 169–175.

(28) Meng, T.; Xie, R.; Ju, X.-J.; Cheng, C.-J.; Wang, S.; Li, P.-F.; Liang, B.; Chu, L.-Y. *J. Membr. Sci.* **2013**, *427*, 63–72.

(29) Cui, J.; Zhang, X.; Liu, H.; Liu, S.; Yeung, K. L. *J. Membr. Sci.* **2008**, *325* (1), 420–426.

(30) Hyun, S. H.; Kim, G. T. *Sep. Sci. Technol.* **1997**, *32* (18), 2927–2943.

(31) Su, C.; Xu, Y.; Zhang, W.; Liu, Y.; Li, J. *Appl. Surf. Sci.* **2012**, *258* (7), 2319–2323.

(32) Zhou, J.; Chang, Q.; Wang, Y.; Wang, J.; Meng, G. *Sep. Purif. Technol.* **2010**, *75* (3), 243–248.

(33) Hu, X.; Yu, Y.; Zhou, J.; Wang, Y.; Liang, J.; Zhang, X.; Chang, Q.; Song, L. *J. Membr. Sci.* **2015**, *476*, 200–204.

(34) Ochoa, N. *J. Membr. Sci.* **2003**, *226* (1-2), 203–211.

(35) Li, Y. S.; Yan, L.; Xiang, C. B.; Hong, L. J. *Desalination* **2006**, *196* (1-3), 76–83.

(36) Yi, X. S.; Yu, S. L.; Shi, W. X.; Sun, N.; Jin, L. M.; Wang, S.; Zhang, B.; Ma, C.; Sun, L. P. *Desalination* **2011**, *281*, 179–184.

(37) Yang, Y.; Zhang, H.; Wang, P.; Zheng, Q.; Li, J. *J. Membr. Sci.* **2007**, *288* (1-2), 231–238.

(38) Nunes, S. P.; Peinemann, K. V. *J. Membr. Sci.* **1992**, *73* (1), 25–35.

(39) Liu, F.; Hashim, N. A.; Liu, Y.; Abed, M. R. M.; Li, K. *J. Membr. Sci.* **2011**, *375* (1-2), 1–27.

(40) Ju, H.; McCloskey, B. D.; Sagle, A. C.; Wu, Y.-H.; Kusuma, V. A.; Freeman, B. D. *J. Membr. Sci.* **2008**, *307* (2), 260–267.

(41) Du, J. R.; Peldszus, S.; Huck, P. M.; Feng, X. *Water Res.* **2009**, *43* (18), 4559–4568.

(42) Hummers, W. S.; Offeman, R. E. *J. Am. Chem. Soc.* **1958**, *80* (6), 1339–1339.

(43) Brodie, B. C. *Philos. Trans. R. Soc. Lond.* **1859**, *149* (0), 249–259.

(44) Kovtyukhova, N. I.; Ollivier, P. J.; Martin, B. R.; Mallouk, T. E.; Chizhik, S. A.; Buzaneva, E. V.; Gorchinskiy, A. D. *Chem. Mater.* **1999**, *11* (3), 771–778.

(45) Liu, Z.; Liu, Q.; Huang, Y.; Ma, Y.; Yin, S.; Zhang, X.; Sun, W.; Chen, Y. *Adv. Mater.* **2008**, *20* (20), 3924–3930.

(46) Li, D.; Müller, M. B.; Gilje, S.; Kaner, R. B.; Wallace, G. G. *Nat. Nanotechnol.* **2008**, *3* (2), 101–105.

(47) Dreyer, D. R.; Park, S.; Bielawski, C. W.; Ruoff, R. S. *Chem Soc Rev* **2010**, *39* (1), 228–240.

(48) Kim, J.; Cote, L. J.; Kim, F.; Yuan, W.; Shull, K. R.; Huang, J. *J. Am. Chem. Soc.* **2010**, *132* (23), 8180–8186.

(49) Buchsteiner, A.; Lerf, A.; Pieper, J. *J. Phys. Chem. B* **2006**, *110* (45), 22328–22338.

(50) Hu, M.; Mi, B. *Environ. Sci. Technol.* **2013**, *47* (8), 3715–3723.

(51) Dong, Y.; Li, J.; Shi, L.; Wang, X.; Guo, Z.; Liu, W. *Chem. Commun.* **2014**, *50* (42), 5586.

(52) Liu, Y.; Zhou, J.; Zhu, E.; Tang, J.; Liu, X.; Tang, W. *Carbon* **2015**, *82*, 264–272.

(53) Jiang, G.; Hu, R.; Wang, X.; Xi, X.; Wang, R.; Wei, Z.; Li, X.; Tang, B. *J. Text. Inst.* **2013**, *104* (8), 790–797.

(54) Li, R.; Chen, C.; Li, J.; Xu, L.; Xiao, G.; Yan, D. *J. Mater. Chem. A* **2014**, *2* (9), 3057.

(55) Huang, Y.; Li, H.; Wang, L.; Qiao, Y.; Tang, C.; Jung, C.; Yoon, Y.; Li, S.; Yu, M. *Adv. Mater. Interfaces* **2015**, *2* (2), 1400433.

(56) Xue, Z.; Wang, S.; Lin, L.; Chen, L.; Liu, M.; Feng, L.; Jiang, L. *Adv. Mater.* **2011**, *23* (37), 4270–4273.

CHAPTER 2

EXPERIMENT

2.1 Materials:

GO was purchased from CheapTubes Inc. Polyvinylidene fluoride (PVDF) membrane was purchased from Sterlitech Corporation. Sodium dodecyl sulfate (SDS) was purchased from Bio-Rad laboratories Inc. Polyamide (PA) and hexadecane (HD) were purchased from Sigma-Aldrich. All chemicals were used as received.

2.2 Fabrication of GO Membranes for Oil/Water Separation:

The high quality single-layered graphene oxide (SLGO) coatings were prepared by facile vacuum filtration process. The schematic process of the fabrication steps was shown in Fig. 3. SLGO powder was first dispersed in DI water, followed by a 30 min sonication (Branson 2510). The SLGO dispersion was centrifuged at 10,000 rpm for different times (Bio Lion XC-H165) to remove large particles/aggregates in the dispersion. The concentration of the resulting SLGO dispersion was tested by UV-vis spectroscopy (Shimadzu UV- 2010PC) with a pre-calibrated curve of GO concentration vs. absorption at 600 nm wavelength in our previous work[1]. Based on the previous result, I obtained the SLGO dispersion after 30 min centrifugation. For GO coating deposition, I filtered the SLGO dispersion onto PA supports with 200-nm pores, PVDF supports with 200-nm pores and ceramic Al_2O_3 supports with 100-nm pores by vacuum filtration (Millipore filtration system). To control the nominal GO coating thickness, we calculated the effective filtration area and added the known amount of GO in its 25-ml dispersion

for filtration, assuming the membrane density is similar to that of graphite (~2.2 g/cm^3).The resulting GO membranes were left on the filtration system for 12 h with vacuum and then ready to use.

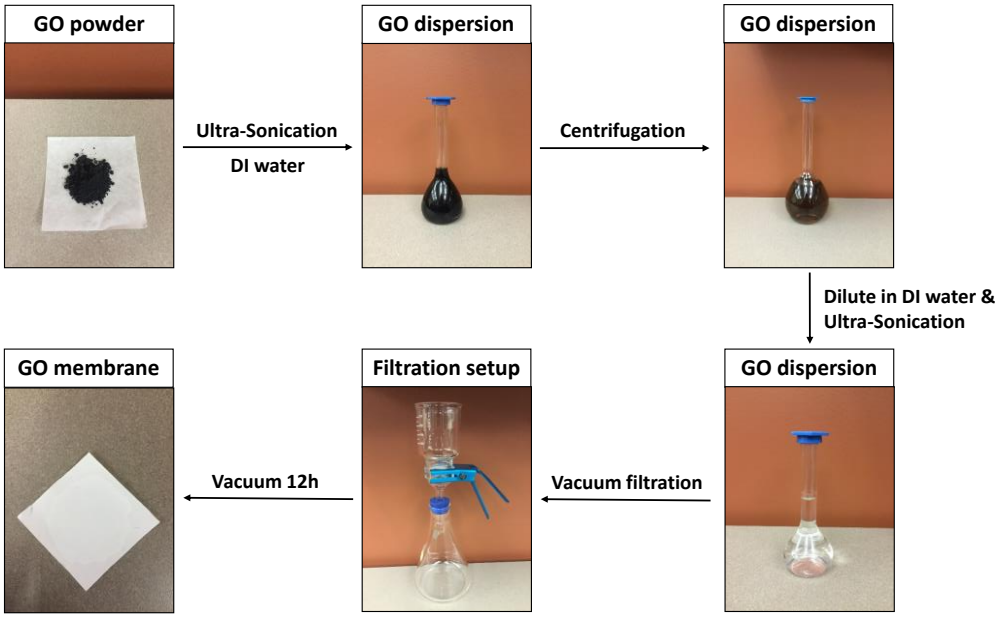

Figure2.1 Fabrication process for GO membranes

2.3 Characterization:

AFM images were obtained on a PicoScan TM 2500 system (Molecular Imagine Corp.) under tapping mode. XPS was conducted for GO coatings (the thickness is 1nm, 2nm, 5nm, respectively) on various substrates on an ESCALab220i-XL instrument (Thermo Fisher Scientific, Inc.) equipped with a monochromated Al Kα X-ray source and hemispherical analyzer with 0.5-eV resolution. FESEM studies were performed using Nova NanoSEM™ 450 scanning electron microscope (FEI Co.). Total organic carbon (TOC) analysis was conducted on a Phoenix 8000 UV-Persulfate TOC Analyzer. Contact angle measurement were taken using a VCP Optima XE system (JC2000C1, Shanghai Zhongchen Digital Technical Spectrum Instruments Co., Ltd., China).

2.4 Preparation of Oil-in-Water Emulsion:

Hexadecane-in-water emulsion was prepared by dissolving 1.5 g of HD (99%) in 2 L of DI water with 100 mg of surfactant, SDS, under ultrasonic mixing for 2 h to produce stable emulsion. Excellent stability of the emulsions was observed visually for at least 48 h. Concentration of this oil/water emulsion was 750 ppm, and the hexadecane droplet size distribution measurements indicated that approximately 75% of the oil droplets have a size in the range of 5–15 μm. Depending on the requirement of experiment, the emulsion was diluted to 750 ppm and 375 ppm.

2.5 Cyclic Separation Tests of Oil-in-Water Emulsion:

A self-designed cross-flow filtration system with an effective permeation area of 3.9 cm^2 was used for oil/water separation experiments, as shown in Fig. 4. The feed side was connected to a diaphragm laboratory pump (KNF lab, NF100KT.18S), which provided a driving force during pure water permeation and water/oil separation. A global valve was connected to the retentate side, which was used to adjust the pressure on the feed side. The flow rate of the feed side was controlled by the pump, and the calibration of the flow rate was shown in Fig. 5. An electronic scale (Ohaus, CS Series) was used to measure the filtrate mass. Before the oil emulsion separation test, the feed side was first connected to a pure DI water tank and a 4-h pure water permeation was conducted to get the initial pure water flux. For the oil-in-water separation, the feed side was switched to an oil/water emulsion tank and the test was conducted for 8 h, during which I took the samples of the permeate (10 mL each) at different times for later TOC measurements. Afterwards, feed side was changed to the DI water tank again while keeping the membrane still in the filtration module; a simple membrane cleaning process was

conducted by flushing the membrane surface with water for 1 h, and the flushing rate during the whole cleaning process was the same as the flow rate used in pure water flux measurement and oil/water emulsion separation test. The 4-h pure-water permeation, 8-h oil/water emulsion separation, and 1-h cleaning process together was considered as an individual cycle. The cycle was repeated 2 times to continuously investigate the effect of

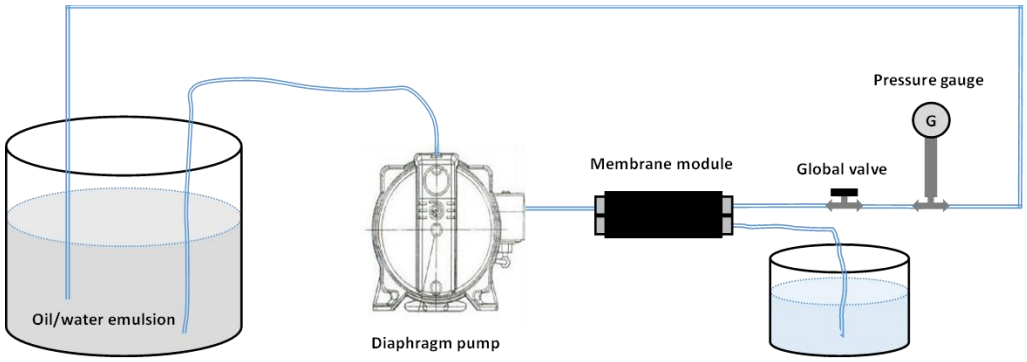

Figure 2.2 Schematic drawing of the cross-flow oil/water filtration system.

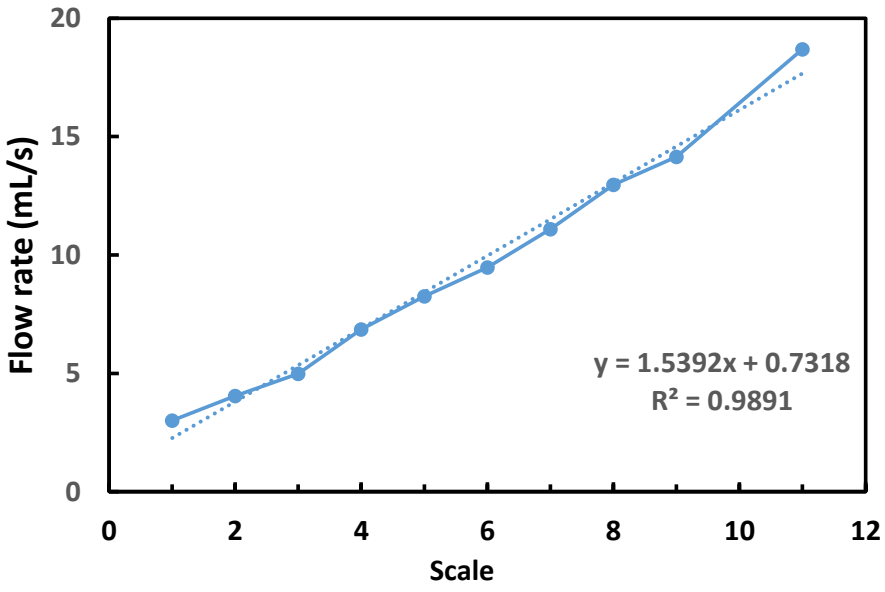

Figure 2.3 The calibration of the pump

GO concentration to the membrane fouling behavior, and repeated 4 times to investigate the recovery capability of GO coating membranes. After that, I did the long time tests

(over 48 h) to investigate the stability of GO coating on the PVDF membrane, and investigated the effect of oil concentration and pressure on the permeate flux during the oil/water separation.

2.6 Water flux, oil rejection and attenuation coefficient measurements

Water flux, oil rejection, and attenuation coefficient were measured by the cross-flow filtration system as showed above. All experiments were conducted with the effective area of 3.9 cm^2 under various pressure drop (0.2 ~ 1) bar at room temperature (20 ~ 22 ^oC). Pure water flux was calculated by:

$$J_V = \frac{V}{S \times t \times P}$$

Where J_V represents the flux through the membrane, V is the permeate volume, S is the membrane active surface area (m^2), and t is the time used to collect the permeate.

The concentration of oil on the feed and permeation sides was analyzed by the Phoenix 8000 UV-Persulfate TOC Analyzer from Teledyne Tekmar. The values of rejection were calculated by:

$$R = \left(1 - \frac{C_P}{C_f}\right) \times 100\%$$

Where C_P and C_f are the concentrations in the permeate and feed, respectively.

The water flux attenuation coefficient (m) of membranes for recovery capability was evaluated by:

$$m = \left(1 - \frac{J_{V,2}}{J_{V,1}}\right) \times 100\%$$

Where $J_{V,1}$ is the initial water flux in the second cycle, after the membrane has been used for 8-h oil/water separation and 1-h water flushing. $J_{V,2}$ is the initial water flux in the third cycle.

References

(1) Li, H.; Song, Z.; Zhang, X.; Huang, Y.; Li, S.; Mao, Y.; Ploehn, H. J.; Bao, Y.; Yu, M. *Science* **2013**, *342* (6154), 95–98.

CHAPTER 3

RESULT AND DISSCUSSION

3.1 AFM

AFM images and average surface roughness of various membranes were illustrated in Fig. 6. Under a scan range of 10 μm × 10 μm, the pure PVDF support had a root-mean-squared roughness (Rq) of 379 nm (Fig. 6 (a)). After coating 1 nm GO on the PVDF surface (Fig. 6 (b)), there was no obvious change of the surface roughness, as the Rq for 1 nm (nominal thickness based on GO amount and density and membrane area;

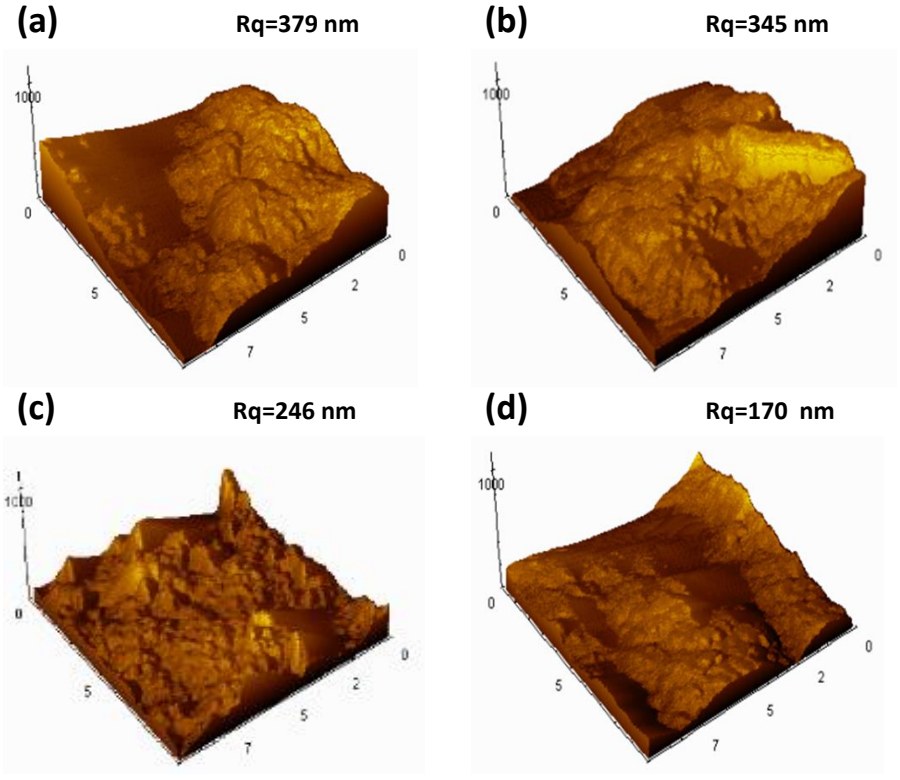

Figure 3.1 AFM images of (a) pure PVDF, PVDF with (b) 1 nm GO coating, (c) 2 nm GO coating, and (d) 5 nm GO coating (three-dimensional, 10 μm × 10 μm).

same for the following thickness) GO coating was 345 nm. This may be because the initially deposited GO just inserted into the pores of PVDF membrane, instead of covering on the surface. However, after coating 2 nm GO on the PVDF support (Fig. 6 (c)), the surface morphology was obviously modified, and the roughness of the GO/PVDF membrane sharply decreased to 246 nm. As I further increased the GO thickness to 5 nm, the surface of the composite GO/PVDF membrane became even smoother, and the Rq value of the membrane decreased to 170 nm (Fig. 6 (d)). This indicates the GO flakes gradually covered the surface of PVDF with the increase of GO amount and totally covered the surface with 5 nm GO coating. These results were consistent with the SEM results that will be discussed below.

3.2 SEM

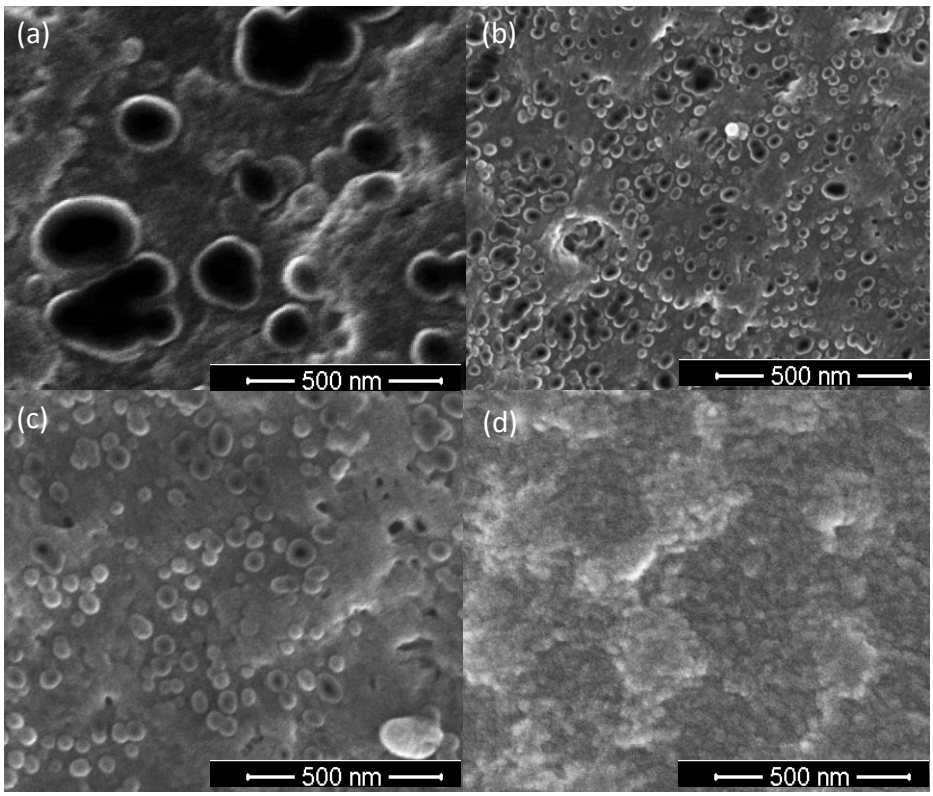

Figure 3.2 FESEM images of (a) pure PVDF, PVDF with (b) 1 nm GO coating, (c) 2 nm GO coating, and (d) 5 nm GO coating.

To visually explore the morphology of the surface of the composite GO/PVDF membrane, field emission scanning electron microscopy (FESEM) was carried out to observe the surface morphology of the PVDF support and PVDF with GO coatings (Fig. 7). The pure PVDF support exhibited a porous structure with approximately 200-nm pores in Fig. 7 (a). However, for the PVDF with 1 nm GO coating (Fig. 7 (b)), I noticed that the average surface pore size of the composite GO/PVDF membrane was much smaller than that of pure PVDF membrane, and the pore size decreased to about 30 ~ 40 nm. But, there was no obvious GO coating noticed on the surface of PVDF support, suggesting that the GO inclusion in the PVDF support might happen during the vacuum filtration. With 2 nm GO coating shown in Fig. 7 (c), it was clearly seen that almost all the black pores were covered by the white bubbles, which suggests accumulation of GO flakes in the pores of PVDF while dense part of the PVDF support was still not completely covered by GO. The 5 nm GO coating showed a planar and continuous surface on the PVDF support, suggesting a complete covering of GO on membrane surface. So with the increase of the GO coating thickness, the continuity and flatness of the membrane improved, which was in good agreement with the AFM results.

3.3 XPS

The surface chemical compositions of GO membranes with different thickness (1, 2 and 5 nm) was explored by XPS. Figure 8 illustrated the typical C 1s spectra of various GO coatings. For pure PVDF membrane (Fig. 8 (a)), the spectra can be deconvoluted into three peaks located at 283.3 eV, 284.6 eV and 289.2 eV corresponding to C-H, C-C and C-F groups. For 1 nm GO coating on the PVDF support (Fig. 8 (b)), five peaks for C-H, C-C, C-OH, O-C=O, and C-F species were obtained, of which C-OH at 285.7 eV and O-

C=O at 288.8 eV indicated the existence of hydrophilic oxygen-containing groups from GO particles. Similar spectral features were also detected on 2 nm and 5 nm GO coating

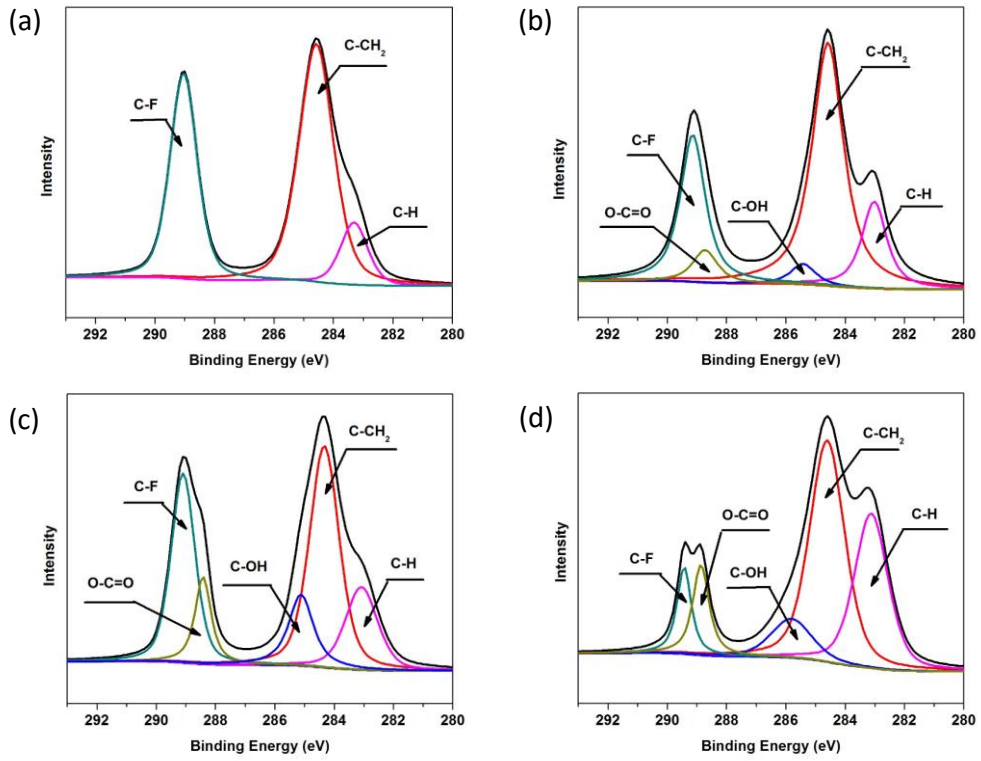

Figure 3.3 XPS spectra of C 1s of (a) pure PVDF, PVDF coating with (b) 1 nm GO, (c) 2 nm GO, and (d) 5 nm GO.

membrane surfaces, which demonstrated GO successfully deposited on the PVDF support. From the Fig. 8 (b) and (c), we can observe that the intensity of O-C=O band increased from 1 nm GO to 2 nm GO coating, indicating the increase of the GO amount on the PVDF surface. Comparison between 5nm (Fig. 8 (d)) and 2 nm GO (Fig. 8 (c)) coatings showed the intensity of C-F band decreased significantly. Apparently, this was caused by the higher coverage of GO. From the SEM images I already knew that the GO totally covered the PVDF surface for 5 nm GO coating membrane, so the intensity of C-F band was expected to decrease.

3.4 Contact angle

Figure 9 showed the water wettability of PVDF membranes before and after coating with GO membranes. Water contact angle of 1 nm, 2 nm and 5 nm GO coatings decreased from 85 ºto 79 º, 78 ºand 68 º, respectively. Fig. 9 (c) showed that with the increasing of the GO coating amount, the contact angle of the GO/PVDF composite membranes decreased, indicating that the surface of the membranes became more and more hydrophilic. The reason why the contact angle slightly decreased for 1 and 2 nm coatings was because GO did not cover all the PVDF support surface and part of the surface was still exposed. When GO completely covered the PVDF support, the contact

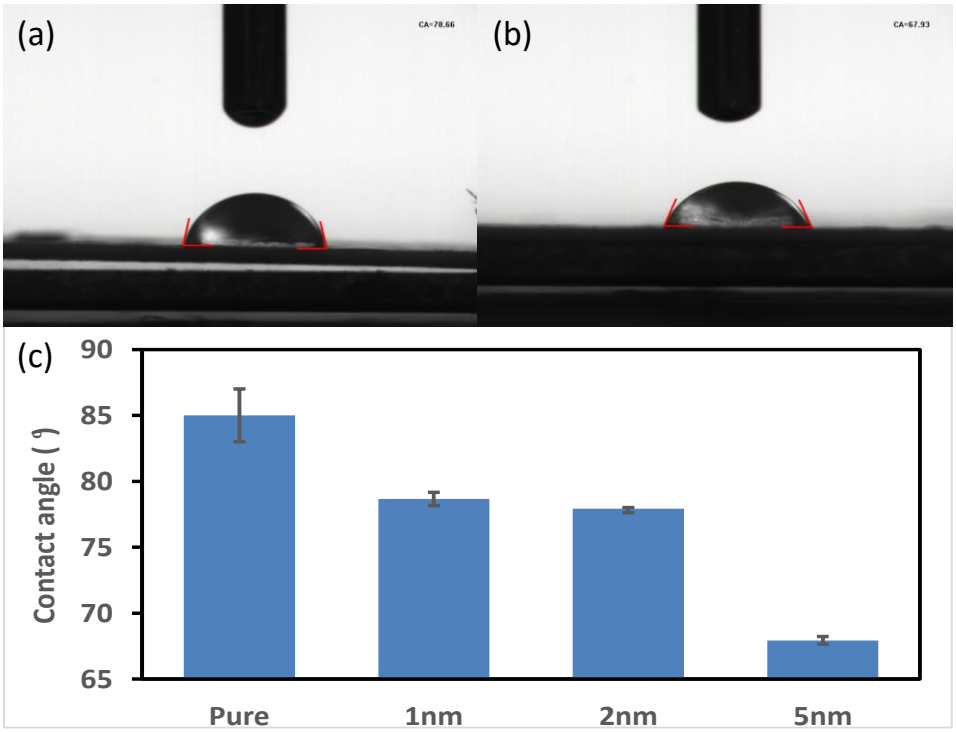

Figure 3.4 Contact angle images (top view) of the PVDF with (a) 1 nm GO coating, (b) 5 nm GO coating, and (c) contact angle versus GO coating thickness.

angle showed a drastic decrease. It could be inferred that the GO coating layer was able to improve the wetting ability of hydrophobic PVDF membrane.

3.5 Mechanism of the GO/PVDF composite membranes

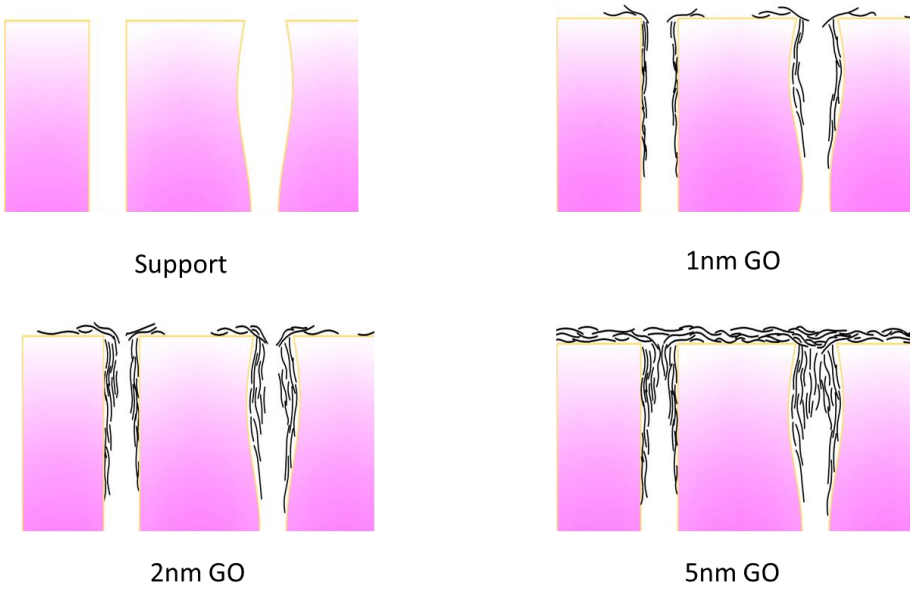

Figure 3.5 The schematic diagrams of the mechanism of GO/PVDF composite membranes.

Based on the above characterizations of AFM, SEM XPS and contact angles, I propose a GO deposition mechanism on PVDF substrate, as shown in Fig. 10. The initial pore size of pure PVDF is around 200-nm. After coating 1-nm nominal SLGO, as the pore size of the composite membrane became much smaller (Fig. 7 (b)) and there was no obvious roughness change based on the AFM results, I assume that SLGO firstly covered/accumulated at the edge of pores, so the pore size of PVDF decreased. But, as the amount of GO flakes was not enough, the pores of PVDF support was not completely covered. For 2-nm GO coating, based on SEM images (Fig. 7 (c)) and the increasing hydrophilicity of the membrane, it seems that most of the pores of PVDF was covered, while part of the PVDF surface was still not completely covered by GO flakes. When the content of GO flakes increased to nominal 5-nm, according to the SEM images (Fig. 7 (d)), XPS (Fig. 8 (d)) and the much smoother surface roughness from AFM (Fig. 6 (d)), it

clearly showed that the whole surface of the PVDF was completely covered by the GO flakes and the hydrophilicity of the membrane increased significantly. This coverage could significantly decrease the flux because of more transport resistance.

3.6 Cyclic separation tests of oil/water emulsion fouling analysis

I conducted cyclic oil/water separation tests using a cross-flow filtration system to explore the separation performance of PVDF with GO coatings. In order to investigate the antifouling performance of the GO coating membranes, two cycles of filtration tests have been designed and the result was shown in Fig. 12. In this experiment, a 375-ppm HD-in-water emulsion stabilized by SDS was used as the feed, and the flow rate was ~10 mL/s. The pressure drop was adjusted to 0.2 bar by the global valve. 4-h pure water permeation was firstly performed, and the water flux decreased rapidly in the first cycle from ~9000 L m^{-2} h^{-1} bar^{-1} to ~650 L m^{-2} h^{-1} bar^{-1}. This may be caused by the oil residues which remained in the cross-flow module after the oil/water separation. Then, I tried to test the pure water flux by a clean dead-end module and found that the trend of the decrease was almost same as the cross-flow module, which was shown in Fig.11. So, I concluded that the sharply decrease may not be caused by the module fouling, but might be caused by the membrane compaction under a pressure drop, which was found in other related PVDF water flux researches[1,2,3]. The reason why the flux was still decreasing during the 3 hour was because the operation pressure drop I used was just 0.2 bar and the flux would use a long time to reach steady state. For the second cycle, I think decline of the pure water flux may be caused by the oil residues fouling, even though the module was cleaned by water flushing for 1 h; some oil droplets may still adsorb on the surface of the PVDF membrane. In the oil/water separation, the initial HD-in-water flux

experienced a rapid decrease because of the deposition and adsorption of the oil droplets on the membrane surface, and then the flux reached a stable value after 3 h. The emulsion flux was ~175 L m^{-2} h^{-1} bar^{-1} through the bare PVDF support, ~360 L m^{-2} h^{-1} bar^{-1} through the PVDF with1 nm GO coating, ~270 L m^{-2} h^{-1} bar^{-1} through the PVDF with

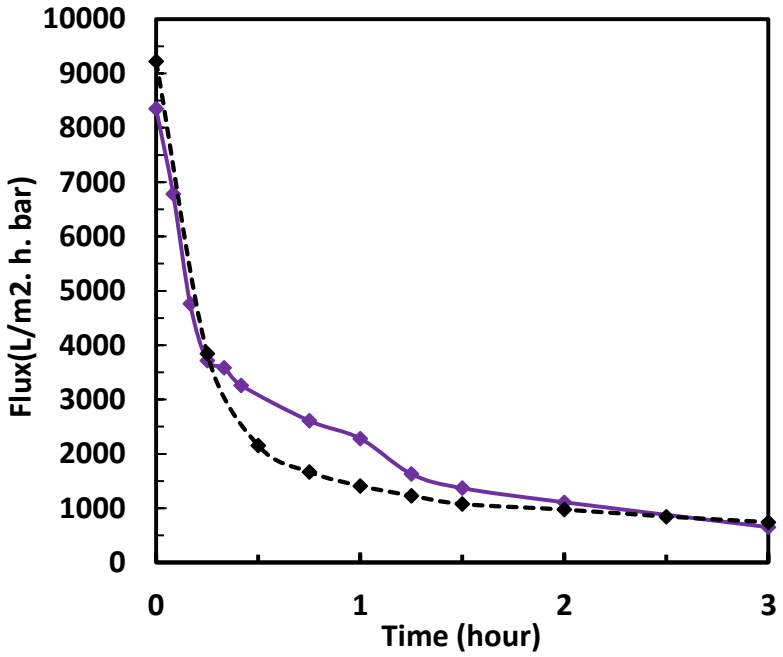

Figure 3.6 Pure water flux for PVDF without any GO coating tested in: (dash line) cross-flow module; (straight line) dead-end module.

2-nm GO coating, and ~110 L m^{-2} h^{-1} bar^{-1} through the PVDF with 5-nm GO coating, respectively. After 1 h water flushing and 4-h pure water permeation, all the membrane exhibited the same stable flux. The excellent antifouling performance of the PVDF with the 1 nm GO coating is because of the low oil adhesion on the membrane surface, which results from the more hydrophilic surface. Based on the two cycles oil/water separation, 1-nm GO coating on PVDF showed the best antifouling performance with the highest stable flux. This can be attributed to the optimized GO coating. The AFM image (Fig. 6 (b)) showed that the roughness of the membrane was almost preserved after coating 1-nm

GO so that the adsorbed oil droplets on the membrane surface was much easier to be washed away by the cross-flow. And based on the result obtained from the SEM images (Fig.7) and XPS spectrum (Fig. 8), with the increase of GO content, the surface of PVDF

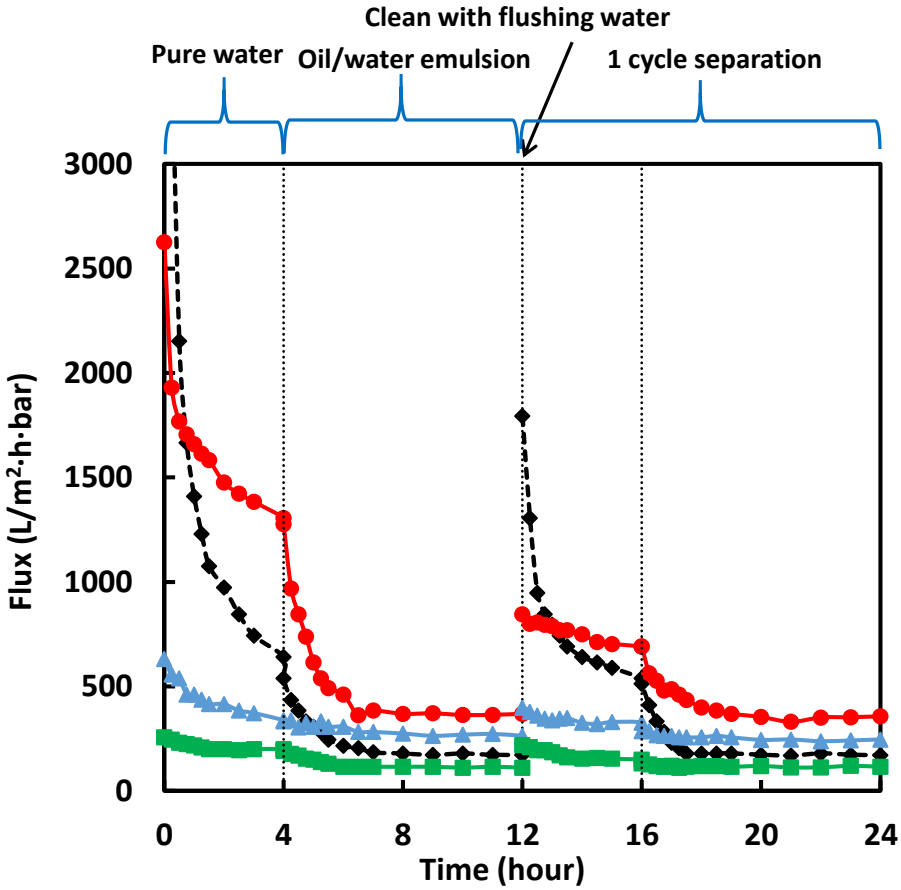

Figure 3.7 Time-dependent flux of GO/PVDF composite membranes: (◊) the pure PVDF support; (●) PVDF with 1 nm GO coating; (Δ) PVDF with 2 nm GO coating; (□) PVDF with 5 nm GO coating.

would be gradually covered by the GO flakes; the resistance between GO flakes could decrease the separation flux when the surface was completely covered. Thus, 1-nm GO coating was the optimal thickness coating for improvement of antifouling performance for oil/water separation. So, I focused on 1 nm GO coating to further investigate the recovery capacity, the effect of the concentration of oil/water emulsion, and the effect of the GO deposition conditions.

3.7 Recovery capacity of the GO/PVDF composite membranes

Recovery capacity of PVDF with 1-nm GO coating was investigated by measuring 4 cycles of pure water + oil/water emulsion filtration, as shown in Fig. 13. Recovery of the pure water flux at the beginning of each cycle was used to evaluate the antifouling performance of the membranes. And during the membrane cleaning, I kept the membrane inside the cross-flow module with ~10 mL/s flow rate. Initial pure water flux through the bare PVDF support was ~ 9000 L m^{-2} h^{-1} bar^{-1} in the first cycle and decreased to ~ 1800 L m^{-2} h^{-1} bar^{-1} in the second cycle after cleaning; in the third cycle, it decreased to ~700 L m^{-2} h^{-1} bar^{-1}; and in the fourth cycle, the flux was only recovered to ~300 L m^{-2} h^{-1} bar^{-1}. This indicated the pure PVDF support experienced severe membrane fouling. However, for PVDF with 1-nm GO coating, the initial pure water flux was ~2600 L m^{-2} h^{-1} bar^{-1} in the first cycle, and after 1 h water flushing in the system, it recovered to ~850 L m^{-2} h^{-1} bar^{-1}. For the following third and fourth cycles, the initial pure water flux was still recovered to ~850 L m^{-2} h^{-1} bar^{-1} and ~860 L m^{-2} h^{-1} bar^{-1}, respectively (the reason why the initial water flux from second cycle just recovered to ~850 L m^{-2} h^{-1} bar^{-1} was attributed to the flow rate used to flushing the membrane surface in the module, which was only ~10 mL/s for 1 h. With the increase of the flushing time, the water flux is expected to recover better). This clearly showed 1-nm GO membrane had almost 100% recovery capacity after cleaning by surface flushing. Decrease of the initial pure water flux in the 2^{nd} - 4^{th} cycles may result from the partially exposed PVDF surface, which leads to unrecoverable fouling after contacting oil/water emulsion in the 1^{st} cycle. For the oil/water separation, the stable permeate flux of pure PVDF support was ~170 L m^{-2} h^{-1} bar^{-1} in the first three cycles; in the fourth cycle, the

stable flux was ~170 L m^{-2} h^{-1} bar^{-1} in the first few hours then began to decrease slowly

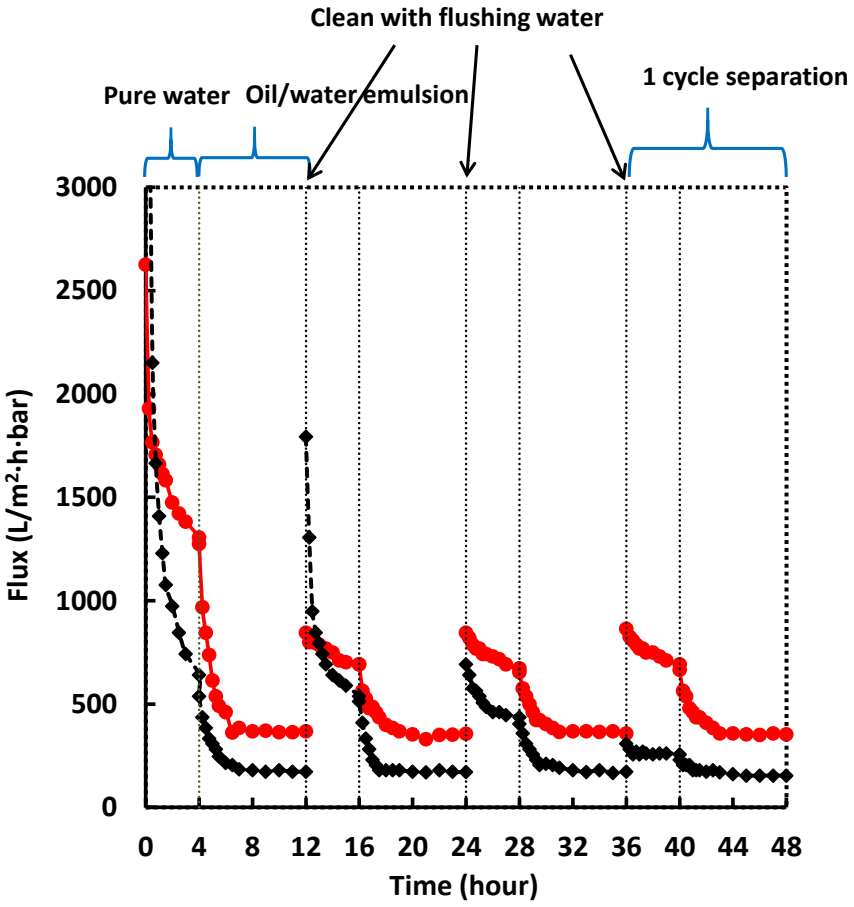

Figure 3.8 Recovery capacity of 1 nm GO/PVDF composite membranes: (◊) the pure PVDF support; (●) PVDF with 1 nm GO coating.

to ~150 L m^{-2} h^{-1} bar^{-1} at last (actually, the flux kept decreasing with time, and I will show this trend in the long time oil/water filtration test of the composite membrane). However, the stable flux of PVDF with 1-nm GO coating was ~360 L m^{-2} h^{-1} bar^{-1} in all four cycles, which was two times of the pure PVDF support. This result showed not only was the pure water flux fully preserved and recovered for each cycle after water flushing, but also the final emulsion flux during oil/water emulsion separation was also preserved, clearly demonstrating its full recovery.

3.8 Effect of vacuum deposition pressure drop for membrane preparation on the antifouling performance

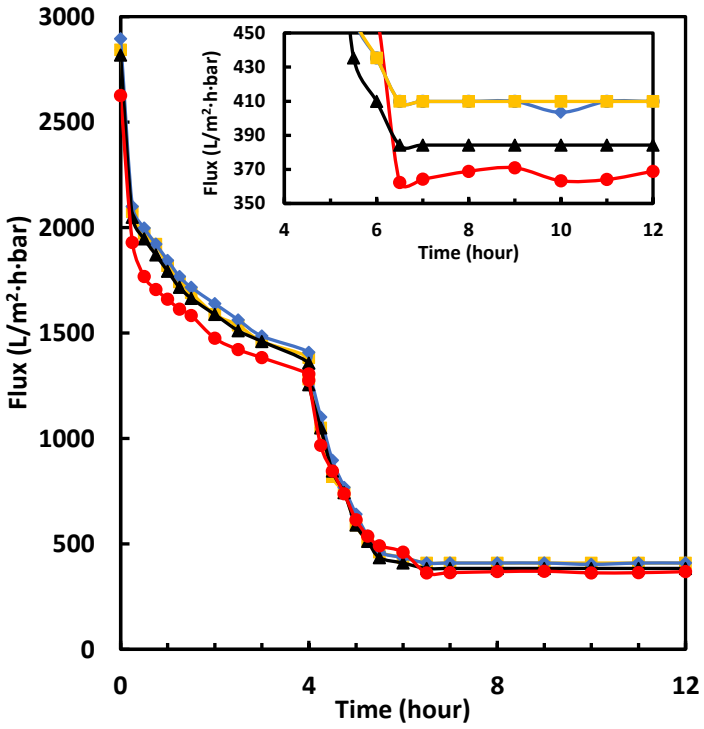

Figure 3.9 Time-dependent flux of 1 nm GO/PVDF coating membranes prepared under different vacuum pressure drop: (◊) 0.1 bar; (□) 0.2 bar; (Δ) 0.6 bar; (●) 0.9 bar. The inset shows the range from 350 to 450 L m^{-2} h^{-1} bar^{-1} of the oil/water separation for the stable flux.

In order to get the optimized antifouling performance of the composite GO/PVDF membranes, I investigated the effect of vacuum deposition pressure drop for membrane preparation on the antifouling performance, since different self-assembly techniques have been shown to induce different GO assembly layer microstructures[4]. Figure 14 showed the antifouling performance of these four membranes; with the decrease of the vacuum pressure drop for membrane preparation, the stable emulsion flux increased from ~360 L m^{-2} h^{-1} bar^{-1} under 0.9 bar to ~380 L m^{-2} h^{-1} bar^{-1} under 0.6 bar, and finally reached ~410 L m^{-2} h^{-1} bar^{-1} under 0.2 and 0.1 bar, which the difference was clearly shown in

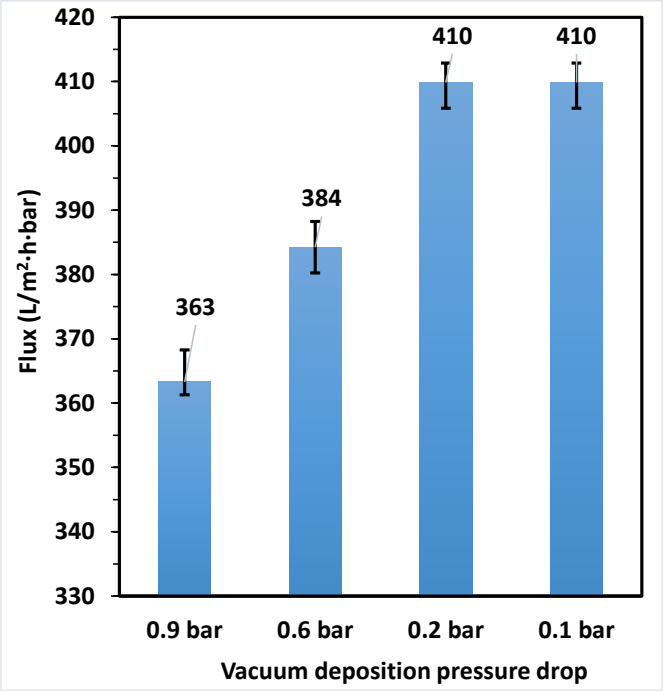

Figure 3.10 Stable emulsion flux of PVDF coating with 1 nm GO membrane with different vacuum pressure drop for membrane preparation.

insert of Figure 14 and Figure 15. The results demonstrated that the vacuum pressure drop for the membrane preparation had big effect on the antifouling performance of the composite membrane. With the decreasing of the vacuum pressure drop, the filtration time of the preparation increased so that the GO coating could better deposited on the PVDF surface and form a higher quality GO coating. For the GO membrane fabricated under -0.2 bar and -0.1 bar, the excellent antifouling performance was attributed to the better GO coating coverage around the pore edges of PVDF membrane at slower deposition rate.

3.9 Effect of GO dispersion concentration for membrane preparation on the antifouling performance

After investigating the effect of vacuum deposition pressure for membrane preparation on the antifouling performance, I continued to explore the effect of the

volume of GO dispersion for the membrane preparation. When studying effect of vacuum deposition pressure, I diluted GO dispersion for 1-nm coating into 40 mL in DI water. To study the GO concentration effect, I diluted the same amount of GO for 1-nm coating into 200 mL and 500 mL DI water, respectively. After the vacuum filtration under 0.9 bar, I did the oil/water separation with these three membranes, which the result was shown in

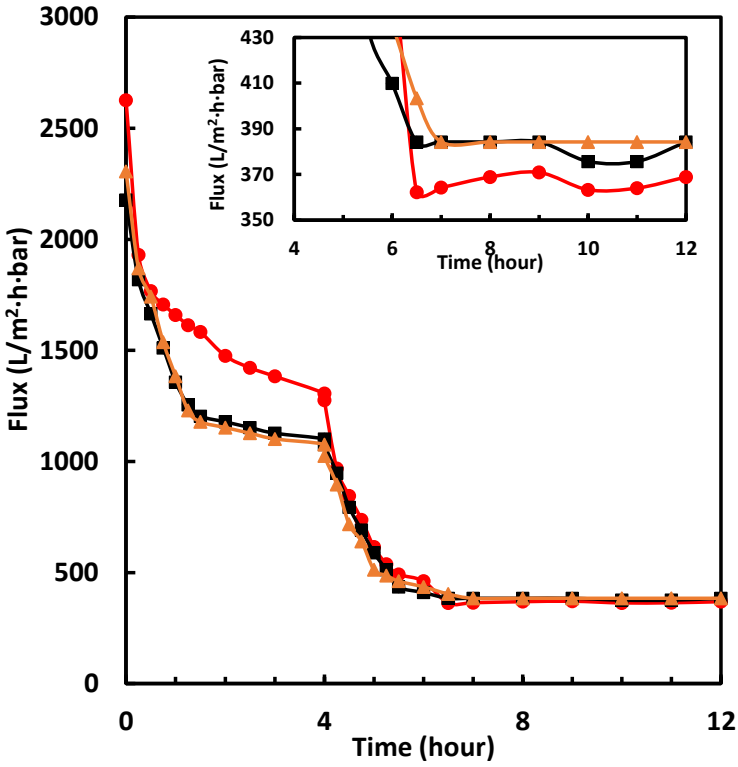

Figure 3.11 Time-dependent flux of 1 nm GO/PVDF composite membranes prepared by different volume of GO dispersion: (●) 40 mL; (□) 200 mL; (Δ) 500 mL

Figure 16. Figure 17 showed that the stable emulsion flux for the 1 nm GO coating membrane improved from ~360 L m^{-2} h^{-1} bar^{-1} to ~385 L m^{-2} h^{-1} bar^{-1} for both 200 mL and 500 mL GO volume. This indicated that the larger volume of GO dispersion or lower GO concentration for membrane preparation had a positive effect on the antifouling performance for oil/water separation. This may result from the better covering of GO

around PVDF pores and thus improved antifouling performance round these GO modified pores. Lower pure water flux for GO coating prepared using 200 and 500 ml dispersion (Fig. 14) may support this, since better covered PVDF pores by GO is expected to have more transport resistance and thus lower water flux.

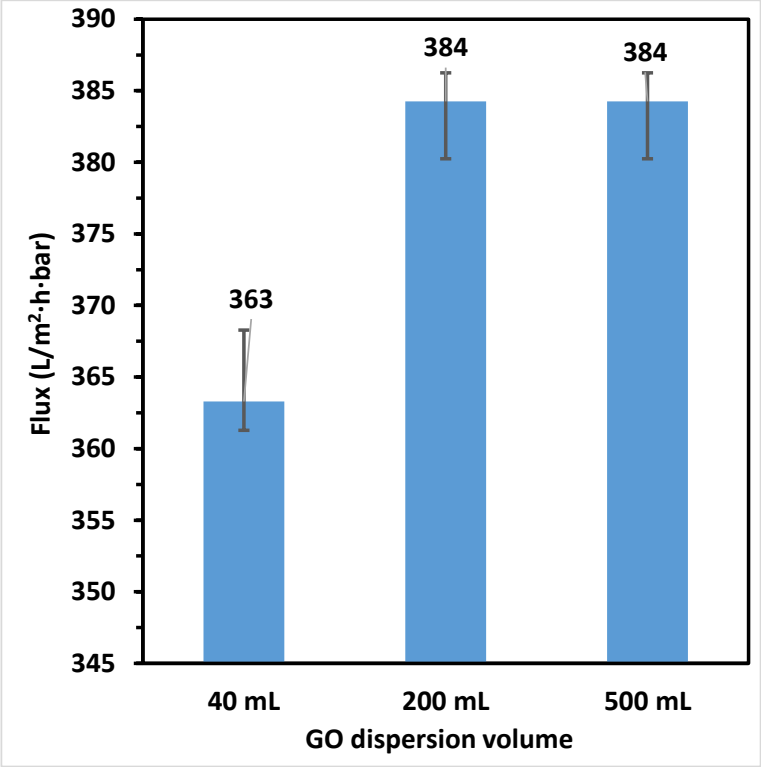

Figure 3.12 Stable emulsion flux of PVDF with 1 nm GO coating deposited from different volume of GO dispersion for membrane preparation.

3.10 Long time stability GO/PVDF composite membranes under cross-flow condition

For the long time stability test for the GO/PVDF composite membranes under cross-flow condition, I chose the 1 nm GO coating membrane prepared under -0.9 bar vacuum pressure and the concentration of the oil/water emulsion was 375 ppm. As shown in Fig. 18, for pure PVDF support, the initial flux of the emulsion was ~900

L m^{-2} h^{-1} bar^{-1}, and then the flux sharply decreased to ~200 L m^{-2} h^{-1} bar^{-1} only in 15 min; flux continued to decrease to ~100 L m^{-2} h^{-1} bar^{-1} within 1 h. For the long time test, the final flux of the pure PVDF was ~50 L m^{-2} h^{-1} bar^{-1} after xx h. For 1 nm GO coated membrane, the antifouling performance was similar to the result I got before, and the flux became stable after 7 h and was ~ 360 L m^{-2} h^{-1} bar^{-1}. This result clearly showed the excellent antifouling performance of GO coated membrane. This not only demonstrated the good stability of the GO/PVDF composite membrane, but also confirmed my assumption for the GO coating mechanism, shown in Fig. 10. Compared with other GO

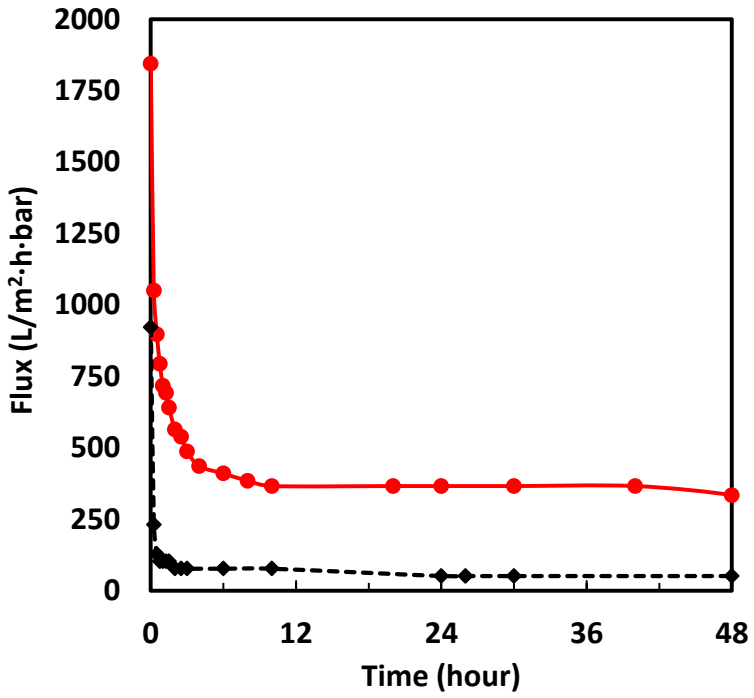

Figure 3.13 Stability test of 1 nm GO/PVDF composite membrane: (◊) the pure PVDF support; (●) PVDF with 1 nm GO coating.

coated membranes for the long time stability test, as the 1 nm GO was deposited into the pores and covered the edges of the pores of PVDF instead of on the PVDF surface, the GO was much harder to be peeled off in the cross-flow system. Based on the result I got from the long time stability test, I did another two experiments to investigate the effect of

operation pressure and oil concentration on the antifouling performance of the oil/water separation, as discussed below.

3.11 Effect of operation pressure drop on the antifouling performance for long time oil/water separation

Figure 19 showed the effect of operation pressure drop on the antifouling performance for long time separation test. When the operation pressure drop was 0.1 and 0.2 bar, the antifouling performance was almost the same. However, for the 0.5 and 1 bar operation pressure, the flux dropped rapidly at the beginning of the separation. This could be due to the formation of an oily layer on top of the membrane at higher pressure drop. For the 0.5 and 1 bar operation pressure drop, the final flux of the membrane was ~120 L m^{-2} h^{-1} bar^{-1} and ~50 L m^{-2} h^{-1} bar^{-1}, respectively after 3 h filtration. Apparently,

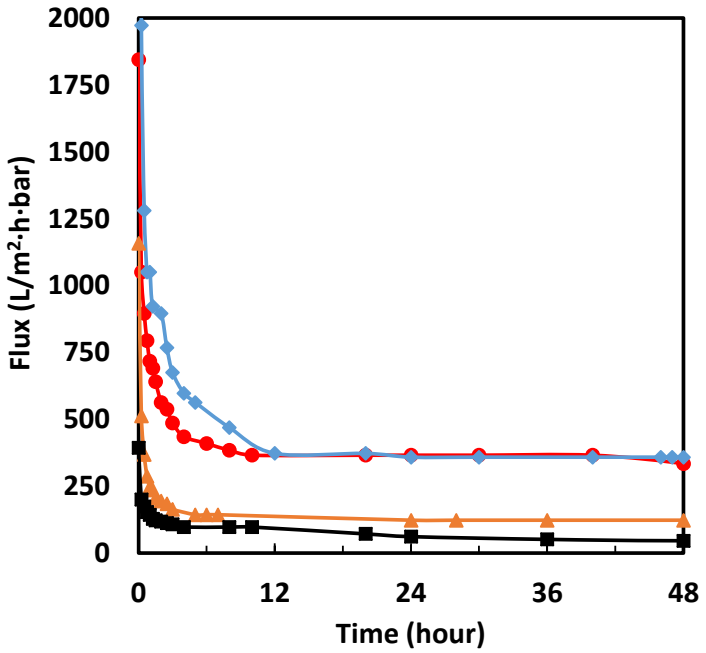

Figure 3.14 Time-dependent flux of 1-nm GO/PVDF composite membranes for long time oil/water separation under different operation pressure drop: (●) 0.1 bar; (◊) 0.2 bar; (Δ) 0.5 bar; (□) 1 bar.

higher pressure drop led to more severe fouling, probably due to stronger adhesion of oil on membrane surface. One viable way to improve the antifouling performance of the composite membrane under high operation pressure may be to increase the cross-flow rate of the feed so that the oil cannot adhere on the surface of the membrane.

3.12 Effect of feed oil concentration on the antifouling performance for long time oil/water separation

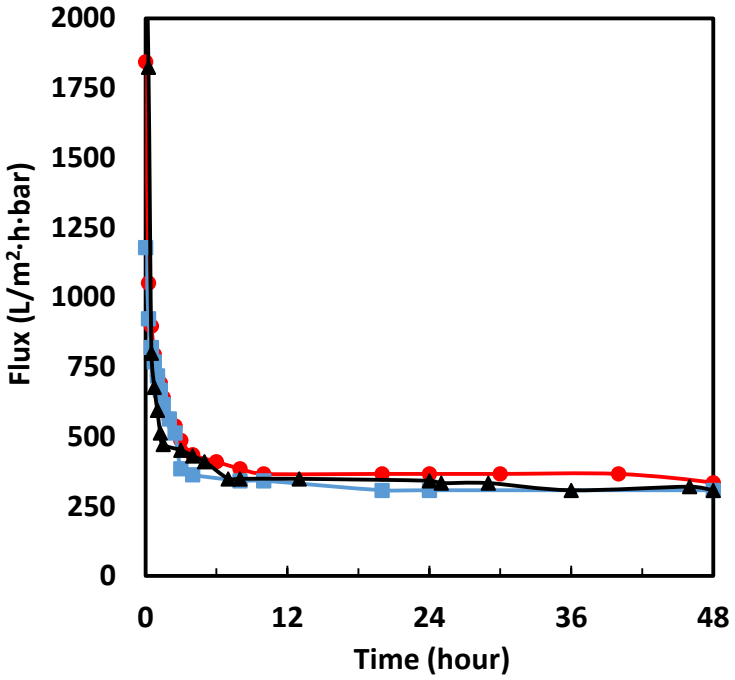

Figure 3.15 Time-dependent flux of 1-nm GO/PVDF composite membranes for long time oil/water separation with different oil concentrations: (●) 375 ppm; (Δ) 750 ppm; (□) 1500 ppm.

Figure 20 showed the effect of the feed oil concentration on the antifouling performance for long time separation test. The antifouling performance for all three oil concentration was similar; the stable emulsion flux after 3 h filtration was around ~310 L m^{-2} h^{-1} bar^{-1} when the feed oil concentration was 750 ppm and 1500 ppm, while the stable flux for 375 ppm was around ~ 360 L m^{-2} h^{-1} bar^{-1}. It might be because the higher oil concentration caused much heavier oil aggregation on the membrane surface, which

led to more severe fouling. Under a fixed cross-flow rate such as ~10 mL/s in this experiment, the flow rate was not high enough to wash all the oil away from the membrane surface, and the oil residues would adhere on the surface and lead to the fouling. So, similar to operation pressure drop, in order to decrease the adhesion of the oil droplets on the membrane surface, increasing the cross-flow rate of the feed may be a viable way to improve the antifouling performance of the composite membrane under high feed oil concentration.

References

(1) Qin, A.; Li, X.; Zhao, X.; Liu, D.; He, C. *J. Membr. Sci.* **2015**, *480*, 1–10.

(2) Zhao, X.; Xuan, H.; Chen, Y.; He, C. *J. Membr. Sci.* **2015**, *494*, 48–56.

(3) Sui, Y.; Wang, Z.; Gao, X.; Gao, C. *J. Membr. Sci.* **2012**, *413-414*, 38–47.

(4) Tsou, C.-H.; An, Q.-F.; Lo, S.-C.; De Guzman, M.; Hung, W.-S.; Hu, C.-C.; Lee, K.-R.; Lai, J.-Y. *J. Membr. Sci.* **2015**, *477*, 93–100.

CHAPTER 4

CONCLUSION

To summarize, this study focused on the GO coating membranes for oil/water separation under cross-flow condition. My results clearly showed the excellent antifouling performance, fully recovery capacity, and good stability of the GO coating membranes. By varieties of characterizations, fundamental separation mechanisms of the GO/PVDF composite membranes was proposed. Cyclic oil/water separation tests demonstrated that great improvement of antifouling performance of the composite membranes was obtained by optimizing the thickness of the GO coatings; 1-nm GO coating showed the best antifouling performance with doubled stable emulsion flux compared with PVDF support. Effect of vacuum deposition pressure drop and GO dispersion concentration for membrane preparation on the antifouling performance was investigated; lower deposition rate led to better covering of the GO coating on the pore edges of PVDF support and thus improved the antifouling performance. At last, I explored the effect of operation pressure drop and feed oil concentration on the antifouling performance for long time oil/water separation, and found that increase of the cross-flow rate was a viable way to improve the antifouling performance of GO composite membranes especially at high operation pressure or high oil concentration. We anticipate that the novel GO coating membranes with optimal thickness have great potential for antifouling oil/water separation to lower the operation cost and elongate membrane service time.